Intraslab earthquakes and 3-D slab structure in Cascadia

Final Report

NEHRP External Grant Award: 03HQGR0097

Kenneth C Creager and Robert S Crosson

Department of Earth and Space Sciences
University of Washington
Seattle, WA 98195-1310
voice: 206-685-2803
fax: 206-543-0489
creager@ess.washington.edu
http://www.ess.washington.edu/creager/

Investigations undertaken

We have developed a method to simultaneously invert first arrival and reflection travel times for 3-D structure, earthquake locations and reflector geometry. The data include times from local earthquakes and several active-source experiments, including the 1998 Wet SHIPS experiment that produced 1200 reflected arrivals and 100,000 first arrivals. The strong reflector is interpreted to be the subducted oceanic Moho. The geographic region containing observed reflected waves has been extended by G. Medema in his PhD work by an analysis of local shallow earthquakes recorded at seismometers of the Pacific Northwest Seismograph Network.

We are also modeling the strong motion seismograms to recover the rupture history of the 2001 Nisqually earthquake. We find that if rupture occurred on the nearly horizontal nodal plane, then it is elongated along strike and the total source rupture could fit within the thickness of the subducting oceanic crust. However, if the rupture occurred on the near vertical nodal plane, the source must have ruptured into the mantle. Unfortunately, aftershocks relocated using a waveform cross-correlation method do not unambiguously determine which is the fault plane.

Determining whether the intraslab events occur within the crust or mantle portions of the slab is not only important for understanding the rupture process of these events, but also for estimating the maximum possible magnitude. Normal-faulting earthquakes confined to the 7 km thick subducted oceanic crust are not likely to exceed the magnitudes of the three large (M6.5-7.1) Cascadia intraslab earthquakes, while allowing a thicker seismogenic zone suggests that much larger earthquakes could occur.

This study investigates the detailed interrelationships among the seismic velocities, earthquake locations, reflector geometry, and the Nisqually fault rupture to better characterize the processes that cause intraslab events such as the Nisqually earthquake.

Results

The results of the wide-angle reflection analysis were published in the journal Science [*Preston, et al.*, 2003] and in Leiph Preston's PhD Dissertation [*Preston*, 2003]. Below is a reformatted version of the Science paper. G. Medema [*2006*] extended the geographic coverage of reflections by analyzing reflected waves from local earthquakes. He concluded that most intraplate earthquakes are in the subducted crust, but that there is a NNE trending lineation of earthquakes that are in the subducted mantle. They coincide with the onshore projection of a pseudofault. We suggest that the propagating rift that formed the pseudofault allowed the circulation of fluids into the uppermost mantle, forming serpentine. As the plate subducts and heats up, serpentine becomes unstable and releases fluids which embrittle the subducting plate allowing earthquakes to occur in the mantle part of the subducting plate.

Intraslab Earthquakes: Dehydration of the Cascadia Slab

Leiph A. Preston, Kenneth C. Creager, Robert S. Crosson
Dept. of Earth and Space Sciences, University of Washington, Seattle, WA, USA

Thomas M. Brocher; U.S. Geological Survey, Menlo Park, CA, USA

Anne M. Trehu; College of Oceanic and Atmospheric Sciences, Oregon State University, Corvallis, OR, USA

We simultaneously invert travel times of refracted and wide-angle reflected waves for 3-Dimensional compressional-wave velocity structure, earthquake locations, and reflector geometry in northwest Washington state. The reflector, interpreted to be the crust-mantle boundary (Moho) of the subducting Juan de Fuca plate, separates intraslab earthquakes into two groups, permitting a new understanding of the origins of intraslab earthquakes in Cascadia. Earthquakes up-dip of the Moho's 45 km depth contour occur below the reflector, in the subducted oceanic mantle, consistent with serpentinite dehydration, while earthquakes located down-dip occur primarily within the subducted crust, consistent with the basalt to eclogite transformation.

The most damaging earthquakes in western Washington have been intraslab events, also known as Wadati-Benioff earthquakes. These include earthquakes in 1949, 1965, and most recently the 2001 moment magnitude (Mw) 6.8 Nisqually event. Although megathrust earthquakes are typically larger in magnitude, intraslab events can be more damaging because they often occur directly beneath population centers, may have shorter recurrence intervals (as in Washington) and tend to have larger seismic energy to moment ratios (*1*) than megathrust events.

The physical mechanisms responsible for intraslab earthquakes in the depth range 30-200 km have been debated for decades. A prominent theory, dehydration embrittlement, asserts that volatiles released during metamorphic dehydration reactions reduce the effective normal stresses across faults, allowing slip (*2,3*). In light of the damaging 2001 Nisqually (Mw6.8), 2001 Geiyo Japan (Mw6.7), and 2001 El Salvador (Mw7.7) intraslab earthquakes, gaining physical insight into the mechanics controlling these earthquakes is important for earthquake hazard estimates and mitigation efforts. The 1998 Seismic Hazards Investigation in Puget Sound (Wet SHIPS)

experiment (*4*) provided an opportunity to investigate the high-resolution structure of the subducting plate in NW Washington and SW British Columbia (*5*).

The Juan de Fuca plate is relatively young and warm (maximum age ~10 My), subducting obliquely at about 40 mm/yr northeastward under Washington and Oregon (Fig. 1). Active intraslab seismicity extends to 60 km depth with some small events reaching depths as great as 100 km (*6*).

The data for the structural inversion consists of 90,000 first-arrival travel times from the wet SHIPS, dry SHIPS, western Cascades, and SW Washington experiments (Fig. S1) (*7,8*), 27,000 first-arrival times from 1400 local earthquakes (200 of which are intraslab events (*9*)), and 1200 secondary arrivals from the Wet SHIPS experiment that are consistent in slowness and travel time with reflections from the Juan de Fuca slab. We developed a non-linear iterative inversion scheme that simultaneously inverts these travel times for earthquake locations, 3-D velocity structure and reflector geometry (*10*). A well-known trade off exists between reflector depth and velocity structure. By including independent first arrival information, we reduce this trade off and extract reliable reflector depths. A smooth velocity model is regularized by minimizing second spatial derivatives of the velocity structure and reflector surface. Travel times of first arrivals are calculated using the Vidale-Hole (*11,12*) 3-D finite-difference code. Theoretical reflected bounce points and travel times are determined by summing calculated travel times from the source and receiver to points on the reflector surface and determining the position and time corresponding to the minimum summed time according to Fermat's principle. Reflected rays are then independently traced from the bounce point to the source and to the receiver. Reflector geometry and the 3-D velocity model are each adjusted to fit the times of reflected waves. This non-linear procedure converges stably after 10 iterations. The final model gives root-mean-square travel-time residuals of 0.09s, 0.12s, and 0.08s for the active-source, earthquake, and reflection data respectively, amounting to variance reductions of 98% and 91% for the active-source and earthquake travel times respectively relative to the standard regional 1-D velocity model (*13*).

We interpret the reflector as the Moho of the subducting Juan de Fuca plate based on two observations. First, the wide-angle reflections are often larger in amplitude than direct arrivals beyond 100 km source-receiver distance and are not observed closer than 55 km, indicative of post-critical reflections associated with an increase in velocities with depth across the reflector. Second, the 3-D model demonstrates increases in velocities with depth in the vicinity of the reflector leading to typical mantle velocities of 8 km/s just below the reflector.

We separate the intraslab earthquakes into two groups: those up-dip (west) of the 45 km reflector contour, and those down-dip of this contour. The up-dip events generally occur at or below the reflector (Figs. 1 and 2). None of the events unambiguously occur above the reflector, considering the combined estimated 2 km uncertainty (*14*) in the earthquake locations and reflector position. In contrast, the down-dip events generally occur at or above the reflector, defining an 8 km thick zone (Fig. 2).

We propose that the up-dip events occur within the subducted oceanic mantle. In the laboratory, serpentinite, a hydrated mantle rock expected to exist in the uppermost oceanic mantle (*15*), becomes brittle under dehydration conditions, forming a visibly wet, clearly defined fault in laboratory samples (*16, 17*). The pressure-temperature (P-T) conditions experimentally determined for this reaction coincide with the P-T conditions predicted for Cascadia in the

vicinity of the up-dip events (*16,18*) (Fig. 3). Thus, we interpret the up-dip events as earthquakes induced by dehydration of serpentinite in the mantle. These mantle earthquakes are confined to a roughly 5 km thick zone with a dip that is slightly shallower than that of the slab Moho, but which is parallel to predicted isotherms (*18*). Dehydration of serpentinite occurs nearly isothermally at these depths (Fig. 3) and thus this behavior is expected (*19*). In contrast, we propose that the down-dip events generally occur in the subducted oceanic crust as a result of embrittlement associated with progressive dehydration (Fig. 3).

The velocity of the rocks within which the earthquakes occur is consistent with this proposed spatial change in earthquake driving mechanism. The up-dip events nucleate in rocks with a velocity of 7.5 to 8.1 km/s whereas the down-dip events nucleate in rocks with a velocity 6.8 to 7.5 km/s (*20*). Deserpentinization of partially serpentinized mantle rocks should result in an upper mantle velocity of ~8 km/s, whereas eclogitization of lower oceanic crust should result in a progressive velocity increase from ~6.8 km/s to 8 km/s (*19*).

Our interpretation requires knowledge of the relative locations of hypocenters, the reflector, and wave speed contours to within a couple kilometers. We have performed specific resolution and error analysis tests to determine our ability to resolve these parameters. Velocity checkerboard tests indicate the necessary resolvability, i.e. little smearing, strong pattern matching and over 50% amplitude return along the cross-section shown in Fig. 2 using 30 km horizontal and 15 km vertical length scales, especially in the top 20 km of the model, but also within the subducting slab where earthquakes occur (Fig. S2). To test whether we would be able to see a low-velocity zone (LVZ) associated with the subducted crust, we perturbed our model by placing an 8 km thick LVZ above and parallel to the reflector, calculated travel times for this model, added random noise to these times and then inverted them (Fig. S3). The inverted model shows only slight smearing of structure and demonstrates returns of over 50% perturbed velocity amplitude throughout the region with earthquakes, and upwards of 75% within the seismic region. Thus, we have the ability to resolve the velocity structure within the slab and at depths shallower than 50 km, and can state that the subducted crust is not a low-velocity wave guide.

In warm subduction zones, such as Cascadia and SW Japan, circumstantial evidence has pointed to intraslab earthquakes occurring generally within the crust. Warm subduction zones lack the lower plane of intraslab seismicity, which is predominant in cold zones where it is clearly occurring within the subducting mantle. Thermal modeling showed that the seismicity cut-off of intraslab seismicity in SW Japan (65km) and in the cold subduction zone of NE Japan (160km) are consistent with the respective depths at which dehydration of the oceanic crust should be complete (*21*). However, intraslab seismicity in SW and NE Japan occur at depths significantly shallower than would be predicted for the basalt to eclogite transformation and indicate that basalt to eclogite reactions cannot explain all the seismicity. In Cascadia, which has a similar thermal structure to SW Japan, the bulk of intraslab seismicity deeper than ~50 km was interpreted to occur within the subducting oceanic crust under SW British Columbia (*22*). Farther to the south, under southwestern Washington, however, the bulk of intraslab seismicity (generally shallower than 40 km) was interpreted as occurring within the subducted mantle (*8*). Our results reconcile these apparently contradictory observations in Cascadia: the down-dip events occur within the subducted oceanic crust and up-dip events occur primarily in the subducted oceanic mantle.

If intraslab earthquakes were purely caused by the basalt to eclogite transformation in the oceanic crust, the intraslab seismicity would be confined to the subducting crust. This

geometrically constrains the maximum expected magnitude of an event to about Mw 7 (*23*). Indeed, the three largest historical intraslab events in 1949, 1965, and 2001 are near this limit. Although we do not observe reflections in the vicinity of these events and, thus, we are uncertain whether these events occur within the oceanic crust or mantle, the wave speeds are well constrained, suggesting these events nucleate near the slab Moho. In Cascadia, earthquakes occur within the oceanic crust and mantle (Fig. 2), geometrically allowing the possibility of a larger event, such as the 2001 Mw 7.7 El Salvador intraslab earthquake.

Fluids released from the down-going plate by the basalt to eclogite or other transformations can have additional consequences. Slow slip events producing 2 cm of thrust-type slip may propagate a few hundred km along strike over a period of a few weeks (*24,25*). These faults appear to coincide with the plate interface and extend down from the down-dip edge of the megathrust locked zone. Coincident in both space and time are recently discovered deep tremor events: non-impulsive sources that are detected at 2 to 6 Hz (*26*) and may be caused by some form of a fluid driven process (*27*). Seven episodic slip events, with a repeat time of about 14 months, have been detected from the Olympic Mountains into southern or central Vancouver Island. The co-location of these deep-creep events with the region interpreted in our model to be undergoing transformation of basalt to eclogite corroborates the hypothesis that these events are controlled by fluid processes. Evidence from several geophysical sources suggests the existence of a serpentinized continental mantle wedge in Cascadia (*28*). This would be expected as fluids released from the subducting plate infiltrate the overlying continental mantle. The lack of a well-defined continental reflector west of the Cascades is consistent with a serpentinized low-velocity mantle wedge. Indeed, wave speeds in our model at depths of 35-45 km in the mantle wedge are less than 7 km/s (Fig. 2), consistent with high concentrations of serpentinite.

Non-Technical Summary

We simultaneously invert travel times of refracted and wide-angle reflected waves for 3-Dimensional compressional-wave velocity structure, earthquake locations, and reflector geometry in northwest Washington state. The reflector, interpreted to be the crust-mantle boundary (Moho) of the subducting Juan de Fuca plate, separates intraslab earthquakes into two groups, permitting a new understanding of the origins of intraslab earthquakes in Cascadia. Earthquakes up-dip of the Moho's 45 km depth contour occur below the reflector, in the subducted oceanic mantle, consistent with serpentinite dehydration, while earthquakes located down-dip occur primarily within the subducted crust, consistent with the basalt to eclogite transformation.

Reports Published

Medema, G. F., Juan de Fuca Subducting Plate Geometry and Intraslab Seismicity, Ph.D. thesis, 97 pp, University of Washington, Seattle, 2006.

Preston, L.A., Simultaneous Inversion of 3D Velocity Structure, Hypocenter Locations, and Reflector Geometry in Cascadia, PhD thesis, Univ. of Washington, Seattle, 2003.

Preston, L.A., K.C. Creager, R.S. Crosson, T.M. Brocher, and A.M. Tréhu, Intraslab earthquakes: Dehydration of the Cascadia slab, *Science*, *302*, 1197-1200, 2003.

Data Availability

The primary data used in this study came from the 1998 Wet SHIPS experiment. Data from this experiment are available from the IRIS DMC (www.iris.washington.edu).

References

1. G. L. Choy, J. L. Boatwright, S. Kirby, *The Radiated Seismic Energy and Apparent Stress of Interplate and Intraslab Earthquakes at Subduction Zone Environments: Implications for Seismic Hazard Estimation* (U.S. Geol. Surv. Open File Report 01-0005, 2001).

2. S. H. Kirby, *J. Geophys. Res.* **92**, 13789 (1987).

3. H. Houston, H. Green, II, *Annu. Rev. Earth Planet. Sci.* **23**, 169 (1995).

4. T. M. Brocher, *et al.*, *Wide-Angle Seismic Recordings from the 1998 Seismic Hazards Investigation in Puget Sound (SHIPS), Western Washington and British Columbia* (U.S. Geol. Surv. Open-File Report 99-314, 1999). The SHIPS experiment consisted of nearly 50,000 airgun sources within the inland waterways of NW Washington and SW British Columbia to over 200 land-based stations.

5. A. M. Trehu, *et al.*, *The Cascadia Subduction Zone and Related Subduction Systems - Seismic Structure, Intraslab Earthquakes and Processes, and Earthquake Hazards*, S. Kirby, K. Wang, S. Dunlop, eds., U.S. Geol. Surv. Open-File Report 02-328 and Geological Survey of Canada Open File 4350 (2002), pp. 25–32.

6. R. S. Ludwin, C. S. Weaver, R. S. Crosson, *Neotectonics of North America*, D. B. Slemmons, E. R. Engdahl, M. D. Zoback, D. D. Blackwell, eds. (Geol. Soc. Am., 1991), Decade Map vol. 1, pp. 77–97.

7. T. M. van Wagoner, *et al.*, *J. Geophys. Res.* **107**, doi:10.1029/2001JB000710 (2002).

8. T. Parsons, *et al.*, *Geology* **26**, 199 (1998).

9. The magnitude range for 95% of these events is between 2.5 and 4.0; however, our data set includes a few events with larger magnitudes, up to 6.8.

10. L. A. Preston, Simultaneous Inversion of 3D Velocity Structure, Hypocenter Locations, and Reflector Geometry in Cascadia, Ph.D. thesis, University of Washington, Seattle (2003).

11. J. Vidale, *Geophysics* **55**, 521 (1990).
12. J. Hole, B. Zelt, *Geophs. J. Int.* **121** (1995).
13. R. Crosson, *J. Geophys. Res.* **81**, 3047 (1976).
14. Material and methods are available as supporting material on Science Online.
15. B. R. Hacker, G. A. Abers, S. M. Peacock, *The Cascadia Subduction Zone and Related Subduction Systems - Seismic Structure, Intraslab Earthquakes and Processes, and Earthquake Hazards*, S. Kirby, K. Wang, S. Dunlop, eds., U.S. Geol. Surv. Open-File Report 02-328 and Geological Survey of Canada Open File 4350 (2002), pp. 133–137.

16. C. Raleigh, M. Paterson, *J. Geophys. Res.* **70**, 3965 (1965).

17. E. H. Rutter, K. Brodie, *J. Geophys. Res.* **93**, 4907 (1988).

18. S. M. Peacock, K. Wang, A. M. McMahon, *The Cascadia Subduction Zone and Related Subduction Systems - Seismic Structure, Intraslab Earthquakes and Processes, and Earthquake Hazards*, S. Kirby, K. Wang, S. Dunlop, eds., U.S. Geol. Surv. Open-File Report 02-328 and Geological Survey of Canada Open File 4350 (2002), pp. 123–126.

19. B. R. Hacker, G. A. Abers, S. M. Peacock, *J. Geophys. Res.* **108**, 2029, doi:10.1029/2001JB001127 (2003).

20. The mean and standard deviations of the compressional-wave velocities at the intraslab earthquake locations, grouped according to the event depth relative to the reflector, are: 7.3±0.3 km/s for events more than 2 km above the reflector, 7.6±0.3 km/s for events within 2 km, and 7.9±0.1 km/s for events more than 2 km below the reflector. See Table S1 for distribution.

21. B. R. Hacker, S. M. Peacock, G. A. Abers, *J. Geophys. Res.* **108**,

10.1029/2001JB001129 (2003).

22. J. F. Cassidy, R. M. Ellis, *J. Geophys. Res.* **98**, 4407 (1993).

23. For example, fault width = 2*crustal thickness = 15km for a fault plane subparallel to slab dip, twice as long as is wide = 30km, having 1.5m slip, rigidity of basalt = 3E10 Pa gives, Mo=rigidity*width*length*slip=2E19 N-m, Mw=2log(Mo)/3-6.06=6.8.

24. H. Dragert, K. Wang, T. S. James, *Science* **292**, 1525 (2001).

25. M. M. Miller, T. Melbourne, D. J. Johnson, W. Q. Sumner, *Science* **295**, 2423 (2002).

26. G. Rogers, H. Dragert, *Science* **300**, 1942 (2003).
27. K. Obara, *Science* **296**, 1679 (2002).
28. T. M. Brocher, T. Parsons, A. M. Trehu, C. M. Snelson, M. A. Fisher, *Geology* **31**, 267 (2003).
29. H. Dragert, R. D. Hyndman, G. C. Rogers, K. Wang, *J. Geophys. Res.*

99, 653 (1994).

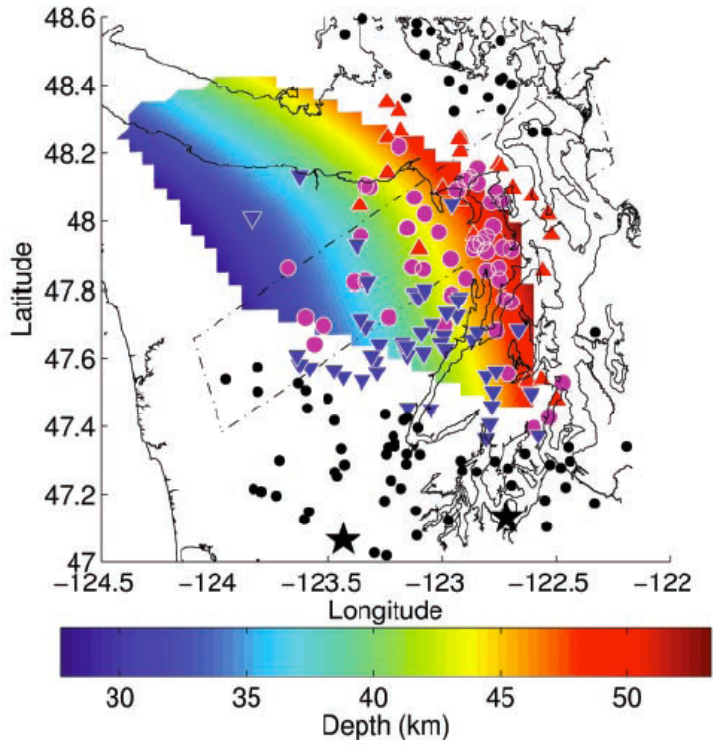

Fig. 1. Depth of reflector surface (colored area) and relocated intraslab earthquakes relative to the reflector [inverted blue triangles: more than 2 km beneath the reflector; maroon circles: within 2 km of the reflector; red triangles: more than 2 km above the reflector; black circles: reflector depth unknown; stars: M_w 5.8 Satsop (**left**) and M_w 6.8 Nisqually (**right**) earthquakes]. The dashed box corresponds to the cross section shown in Fig. 2 and is parallel to the relative plate motion direction.

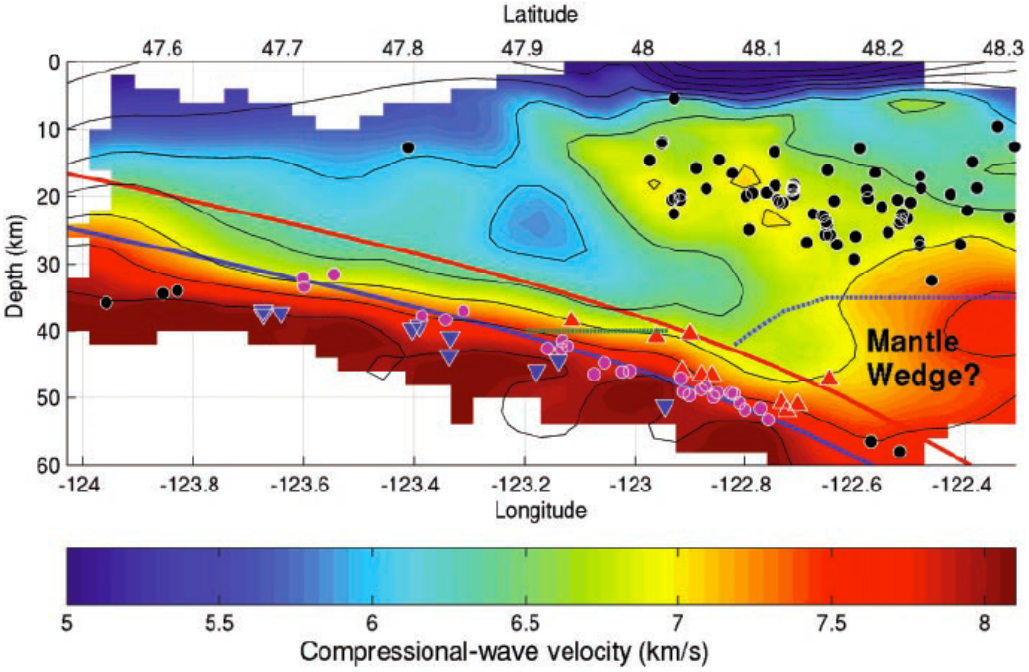

Fig. 2. Interpreted cross section (see dashed box in Fig. 1) showing compressional velocities (contoured at 0.5-km/s intervals), relocated seismicity (black circles: continental crustal events; colored symbols: intraslab events coded as described in Fig. 1), and Moho reflector (blue line). Interpreted top of subducting plate (red line) is drawn 7 km above reflector. The region between these lines is interpreted to be the subducting oceanic crust, composed of basalt above 40-km depth (horizontal green line) and beginning to transform to eclogite below. Subducting mantle is below the blue line. Low velocities in the mantle wedge imply the presence of serpentinite. There is no vertical exaggeration.

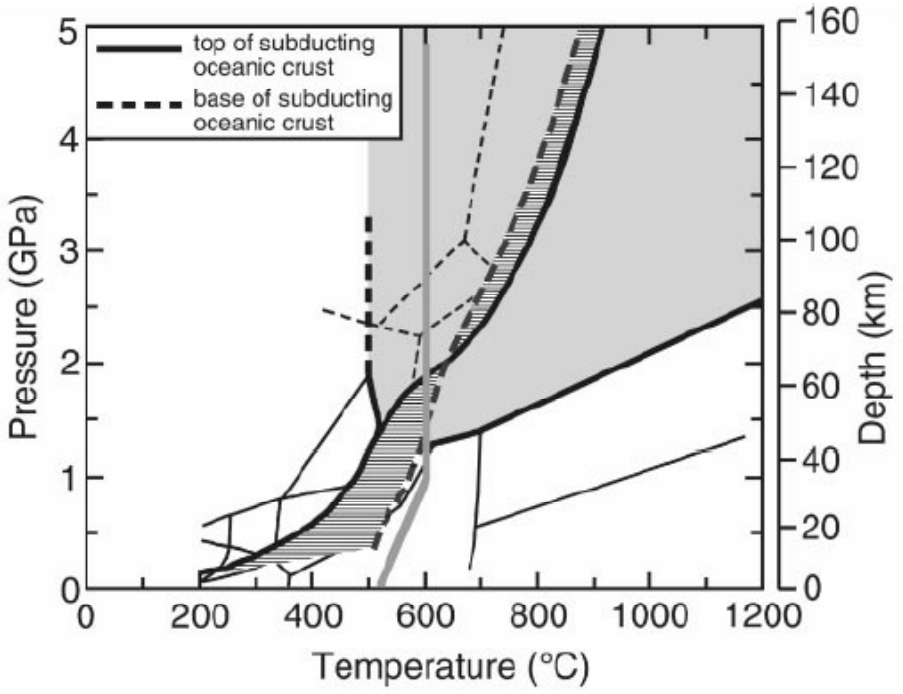

Fig. 3. Simplified phase diagram for the basalt (white)-to-eclogite (gray) transformation and serpentinite dehydration reaction (gray line) (*19*) overlaid with the calculated pressure-temperature path for the Cascadia slab (hashed). Note that, in the vicinity of the Cascadia geotherm, the basalt-to-eclogite transformation occurs at nearly constant pressure, independent of temperature, whereas the serpentinite dehydration reaction occurs at nearly constant temperature, independent of pressure. A geotherm just below the Moho would lie to the right (hotter) of the dashed line and, thus, would intersect the serpentinite dehydration line at a shallower depth. [Modified from (*18*)]